J Biochem Technol (2025) 16(4): 107-115
https://doi.org/10.51847/lxvYlZutW9
ISSN: 0974-2328

# Pharmacophore Screening, Molecular Docking, and ADME-Tox Evaluation of Marine Natural Products as Potential SARS-CoV-2 Mpro Inhibitors

**Elaine Joy Torre, Junie Billones***

Received: 17 September 2025 / Received in revised form: 27 November 2025, Accepted: 29 November 2025, Published online: 23 December

## Abstract

The SARS-CoV-2 main protease (Mpro), a cysteine protease essential for viral polyprotein processing and replication, remains a validated molecular target for the development of COVID-19 therapeutics. This study employed an integrated in silico drug discovery workflow combining structure-based and ligand-based pharmacophore modeling, large-scale virtual screening, molecular docking, and ADME–Tox prediction to identify potential marine natural product inhibitors of Mpro. A dataset of over 30,000 compounds from the Comprehensive Marine Natural Products Database (CMNPD) was screened using a ligand-based pharmacophore derived from 30 reported Mpro inhibitors and a structure-based pharmacophore generated from the Mpro–boceprevir co-crystal complex. Initial screening yielded 900 ligand-based and 1,259 structure-based hits. Subsequent molecular docking analysis identified 88 and 98 compounds, respectively, exhibiting more favorable binding energies than the reference inhibitor boceprevir. Lead candidates, including versixanthone F and penicillixanthone B, demonstrated critical interactions with the catalytic residue Cys145 within the active site. ADME–Tox filtering further prioritized purealin D, pseudogymnoascin A, and pseudogymnoascin B, although pharmacokinetic limitations were noted. Additional non-hepatotoxic candidates such as homodolastatin 3 and dolastatin 3 emerged as promising scaffolds for structural optimization and future experimental validation.

**Keywords:** SARS-CoV-2 main protease ($M^{pro}$), Marine natural products, Pharmacophore screening, Molecular docking, ADME-Tox evaluation

## Introduction

The COVID-19 pandemic has profoundly affected global health and disrupted economies worldwide. SARS-CoV-2, the causative agent, infects alveolar cells by binding its spike protein to the angiotensin-converting enzyme 2 (ACE2) receptor, with activation by the transmembrane serine protease 2 (TMPRSS2) facilitating viral entry (Jackson *et al*., 2022). Like other RNA viruses, SARS-CoV-2 evolves rapidly, giving rise to variants such as Alpha, Beta, Gamma, Delta, and Omicron, which complicate disease management (Cascella *et al*., 2023). Typical symptoms include fever, cough, and loss of smell or taste.

Due to its essential role in viral replication, the SARS-CoV-2 main protease ($M^{pro}$ or 3-chymotrypsin-like protease, 3CLpro) is a key target for antiviral drug discovery. $M^{pro}$ processes polyproteins translated from viral RNA, releasing nonstructural proteins, including RNA-dependent RNA polymerase (RdRp), necessary for genome replication and transcription (Zhang *et al*., 2020; Gurung *et al*., 2021). The enzyme's catalytic cycle involves cysteine-mediated acylation and deacylation, which enables successive cleavage of viral polyproteins (Ramos-Guzmán *et al*., 2020). Inhibiting $M^{pro}$ disrupts viral multiplication and therefore offers a promising therapeutic approach.

Researchers worldwide have employed computer-aided drug discovery (CADD) to identify potential SARS-CoV-2 therapeutics. Pharmacophore modelling and virtual screening have led to the identification of candidate compounds from diverse sources (Gaudêncio & Pereira, 2020; Iheagwam & Rotimi, 2020; Shehroz *et al*., 2020). Several approved drugs, such as lopinavir, ritonavir, and ivermectin, as well as the $M^{pro}$ inhibitor PF-07321332 (nirmatrelvir), have shown promise (Caly *et al*., 2020; Gurung *et al*., 2021; Reina & Iglesias, 2022). CADD accelerates drug discovery by providing molecular insights and reducing the cost and time associated with experimental methods (Tomar *et al*., 2019).

Virtual screening approaches include ligand-based and structure-based strategies. Ligand-based screening generates a pharmacophore from known active ligands when no receptor structure is available, whereas structure-based screening derives a pharmacophore from the target's binding site (Sharma *et al*., 2021). These pharmacophores, representing the key steric and electronic features required for optimal target binding, guide the selection of candidate molecules (Yang, 2010). Top-scoring hits are then subjected to molecular docking to predict their binding affinity and orientation within the active site (Meng *et al*., 2011). This study employs both ligand-based and structure-based pharmacophore screening of marine natural products, followed by molecular docking and ADME-Tox evaluation, to identify novel SARS-CoV-2 $M^{pro}$ inhibitors for potential therapeutic development.

**Elaine Joy Torre, Junie Billones***
Department of Physical Sciences and Mathematics, College of Arts and Sciences, University of the Philippines Manila, Ermita, Manila, Philippines.

***E-mail:** jbbillones@up.edu.ph

## Materials and Methods

All computational experiments were performed on a desktop running Microsoft Windows 7 Home Basic 64-bit with an Intel® Core™ i7-3770 CPU and 8 GB RAM. All computations used Accelrys Discovery Studio (DS) 2.5 (now BIOVIA, https://www.3ds.com).

*Structure-Based Pharmacophore Model Generation*

The crystal structure (1.60 Å resolution) of the SARS-CoV-2 main protease ($M^{pro}$) complexed with Boceprevir (PDB ID: 7C6S) was obtained from the RCSB Protein Data Bank. The structure was prepared and optimized in DS 2.5 using the *Prepare Protein* protocol to remove solvent molecules and other heteroatoms. Energy minimization was performed with the CHARMM force field using the smart minimizer algorithm for a maximum of 200 steps at an RMS gradient of 0.001 kcal/mol·Å.

The Boceprevir binding site was identified, and a binding-site sphere was generated around the catalytic residue Cys145 (Fu *et al*., 2020) to define the active site for subsequent analyses. To assess structural changes after preparation, the original and minimized protein structures were superimposed using DS 2.5. The Root Mean Square Deviation (RMSD), which measures the average atomic displacement between two structures, was calculated. In general, the acceptable RMSD threshold value is 2.0 Å (Maia *et al*., 2020).

The *Interaction Generation* protocol was applied to create a pharmacophore model representing key steric and electronic features within the active site (Yang, 2010). To limit the number of features to fewer than 30, the *Cluster Features* and *Keep Only Cluster Centers* protocols were used.

*Ligand-Based Pharmacophore Model Generation*

Thirty known SARS-CoV-2 $M^{pro}$ inhibitors, previously tested in the same biological assay (Macip *et al*., 2022), were collected. Two-dimensional structures were either drawn using MarvinSketch or obtained as SDF files. The *Prepare Ligands* protocol generated isomers, tautomers, and 3D conformations, removed duplicates, and minimized energy using CHARMM (1,000 steps; RMS gradient 0.001 kcal/mol·Å) (Billones *et al*., 2016).

The ligands were subjected to the *Common Feature Pharmacophore Generation* protocol, and the highest-ranked model was selected. Robustness was evaluated by generating a Receiver Operating Characteristic (ROC) curve using a database of known actives and inactives. The AUC (area under the ROC curve) quantifies the ability of a model to discriminate between classes; an AUC of 0.5 corresponds to random chance, 1.0 corresponds to perfect discrimination, and intermediate values are generally regarded as acceptable for predictive ability (Çorbacıoğlu & Aksel, 2023).

*Virtual Screening*

A library of over 30000 compounds from the *Comprehensive Marine Natural Products* database (CMNPD) was downloaded as SDF files (Lyu *et al*., 2021). Ligands were prepared and energy-minimized using the *Prepare Ligands* protocol. The Lipinski filter was disabled to accommodate natural products, which often exhibit drug-like activity despite Lipinski's rule violations (Billones *et al*., 2013).

Virtual screening was carried out with the *Screen Library* protocol using both the structure-based and ligand-based pharmacophores. Rigid fitting was applied first, followed by flexible fitting to refine hit selection (Costa *et al*., 2022; Dipalma *et al*., 2022; Sugimori *et al*., 2022; Zhao *et al*., 2022).

*Molecular Docking*

Top-scoring compounds (≥2.5 fit for rigid and ≥3.0 for flexible fitting in structure-based, and ≥2.5 rigid and ≥2.9 flexible in ligand-based screening) were subjected to molecular docking using the *Dock Ligands (CDOCKER)* protocol. CDOCKER employs a CHARMM-based molecular dynamics algorithm, allowing ligands to move within the receptor's active site (Wu *et al*., 2003).

Binding affinities were computed using the *Calculate Binding Energy* protocol. Compounds with more negative binding energies than the reference ligand Boceprevir were prioritized as top hits.

*ADME-Tox Evaluation*

Compounds with superior docking scores were further evaluated for Absorption, Distribution, Metabolism, and Excretion (ADME) and toxicity (Tox) profiles. Using DS 2.5 *ADMET* and *TOPKAT* protocols, the following were predicted: aqueous solubility, CYP2D6 inhibition, hepatotoxicity, human intestinal absorption, plasma protein binding, developmental toxicity potential, mutagenicity (Ames test), carcinogenicity, and aerobic biodegradability.

Additionally, SwissADME was used to assess lipophilicity, PAINS alerts, and synthetic accessibility. Compounds combining favorable binding energies and acceptable ADME-Tox profiles were identified as potential SARS-CoV-2 $M^{pro}$ inhibitors.

## Results and Discussion

*Structure-Based Pharmacophore Generation*

The 1.60 Å crystal structure of the SARS-CoV-2 main protease complexed with boceprevir (PDB ID: 7C6S) was retrieved from the RCSB Protein Data Bank (https://www.rcsb.org/structure/7C6S). Protein preparation involved standard pre-processing steps: insertion of missing atoms, modeling of incomplete loop regions, removal of alternate conformations and water molecules, standardization of atom names, and protonation of titratable residues based on predicted pK values (García *et al*., 2023; Stoev *et al*., 2023; Yurievna *et al*., 2023).

Energy minimization was then performed with the CHARMM force field using the *Smart Mnimizer* algorithm (200 steps, RMS gradient = 0.001) via the conjugate-gradient method (Fletcher & Reeves, 1964). This step optimizes geometry to the lowest local

free-energy state, relieving steric clashes. The potential energy decreased from –12238.7 to –18970.4 kcal/mol. Structural deviation between the raw and minimized proteins was evaluated by superimposition of their Cα atoms. The root-mean-square deviation (RMSD) was 0.659 Å, well within the threshold value of 2.0 Å (Maia *et al*., 2020), indicating that the preparation did not significantly alter the protease's overall conformation **(Figure 1)**.

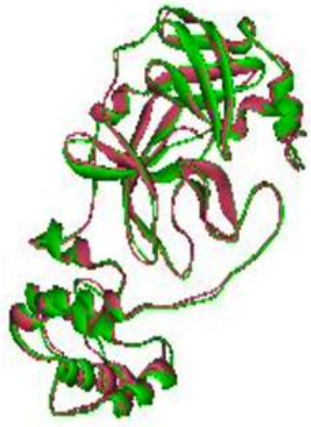

**Figure 1.** Superimposed ribbon structures of the raw (green) and prepared/minimized (dark pink) SARS-CoV-2 main protease crystal structures, showing an RMSD of 0.659 Å.

The binding site was defined from the boceprevir co-crystal complex (Fu *et al*., 2020). A site sphere of radius 9.362 Å was generated (center coordinates: x = –19.63, y = –27.452, z = 0.735) to encompass key catalytic residues Gly143, Cys145, His41, His164, and Glu166 **(Figure 2)**.

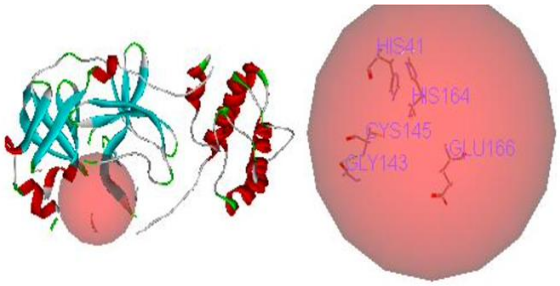


**Figure 2.** Solid ribbon diagram showing the protein's active site (left) and the key amino acid residues—Gly143, Cys145, His41, His164, and Glu166—within the active site (right).

To validate the docking procedure, boceprevir was removed and redocked using the CDOCKER protocol. The redocked pose showed an RMSD of 1.059 Å relative to the crystal conformation—an acceptable value for pose reproduction (Cosconati *et al*., 2010). Key interactions, including hydrogen bonds between Cys145 and the ligand's carbonyl oxygen and between Glu166 and the ligand, were preserved. Minor differences, such as an additional hydrogen bond with Gln189, were observed.

Using the *Interaction Generation* tool in DS, a receptor-based pharmacophore comprising 22 features was created: seven hydrogen-bond acceptors, eight donors, and seven hydrophobic sites. These features capture the key interaction motifs of boceprevir and were used to screen the CMNPD.

*Ligand-Based Pharmacophore Generation*

Thirty known SARS-CoV-2 main protease inhibitors (Macip *et al*., 2022) were built in MarvinSketch and processed with the *Prepare Ligands* protocol to remove duplicates, enumerate tautomers/isomers, and generate 3D conformers. Energy minimization was then performed using the CHARMM force field.

Feature Mapping identified 906 potential pharmacophoric features, the most frequent being hydrogen-bond acceptors and lipid acceptors. *Common Feature Pharmacophore Generation* protocol with the *HipHop* algorithm produced ten hypotheses. One hydrophobic feature and two hydrogen-bond acceptors made up the top-ranked model.A receiver operating characteristic (ROC) curve assessed the model's ability to discriminate active from inactive compounds. The area under the curve (AUC) was 0.667, indicating modest predictive ability (Çorbacıoğlu & Aksel, 2023).

*Virtual Screening*

Databases were pre-processed with *Prepare Ligands* and screened against the receptor- and ligand-based pharmacophores using rigid and flexible fitting. In the structure-based approach, compounds with rigid-fit values ≥2.5 were subsequently subjected to flexible fitting (fit value ≥3.0), which reduced the CMNPD entries to 1259. In the ligand-based approach, rigid-fit cut-off of 2.5 and flexible-fit cut-off of 2.9 yielded 900 compounds. These filtered hits proceeded to molecular docking.

*Molecular Docking*

Molecular docking with CDOCKER predicted ligand orientation and binding affinities. Boceprevir, used as a reference, had a binding energy of –277.2 kcal/mol. In structure-based screening, eighty-eight CMNPD compounds showed more negative binding energies than boceprevir; the top five are listed in **Table 1**. The best hit, CMNPD26286 (versixanthone F), displayed a binding energy of –444.2 kcal/mol and formed hydrogen bonds with Gly143 and Cys145, carbon–hydrogen bonds with Glu166, Met165, and Asn142, and hydrophobic contacts with Met165, Leu167, Pro168, and Met49 **(Figure 3)**. The other top-ranking candidates were blennolide I (CMNPD26372), versixanthone D (CMNPD26284), versixanthone B (CMNPD26282), and adenochromine A (CMNPD1635), all of which also displayed favorable docking energies and key interactions within the $M^{pro}$ active site.

**Table 1.** Top 5 structure-based hits with their structures, binding energies, and fit values.

| Index | Compound ID | Structure* | Binding Energy (kcal/mol) | Fit Value (Rigid) | Fit Value (Flexible) |
|---|---|---|---|---|---|

| | | | | | |
|---|---|---|---|---|---|
| **1** | CMNPD26286 | 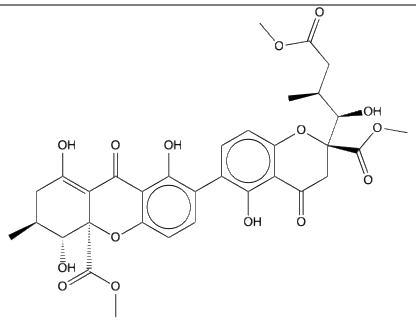 | –444.2 | 2.62 | 3.78 |
| **2** | CMNPD26372 | 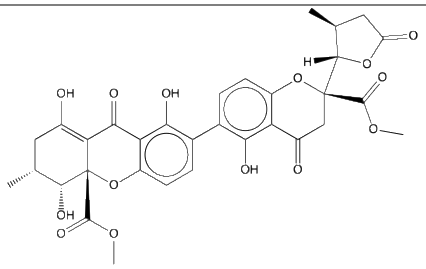 | –429.2 | 2.54 | 3.60 |
| **3** | CMNPD26284 | 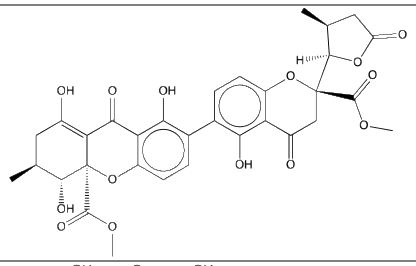 | –396.6 | 2.68 | 3.53 |
| **4** | CMNPD26282 | 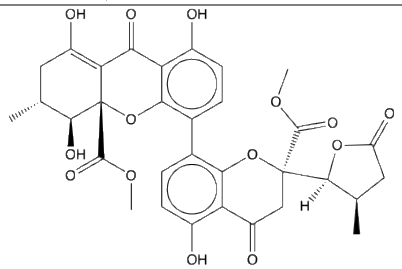 | –395.1 | 2.62 | 3.87 |
| **5** | CMNPD1635 | 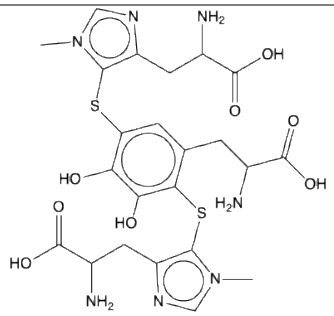 | –390.1 | 2.83 | 3.27 |
| – | Boceprevir (reference) | 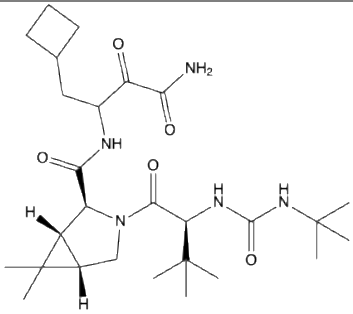 | –277.2 | – | – |

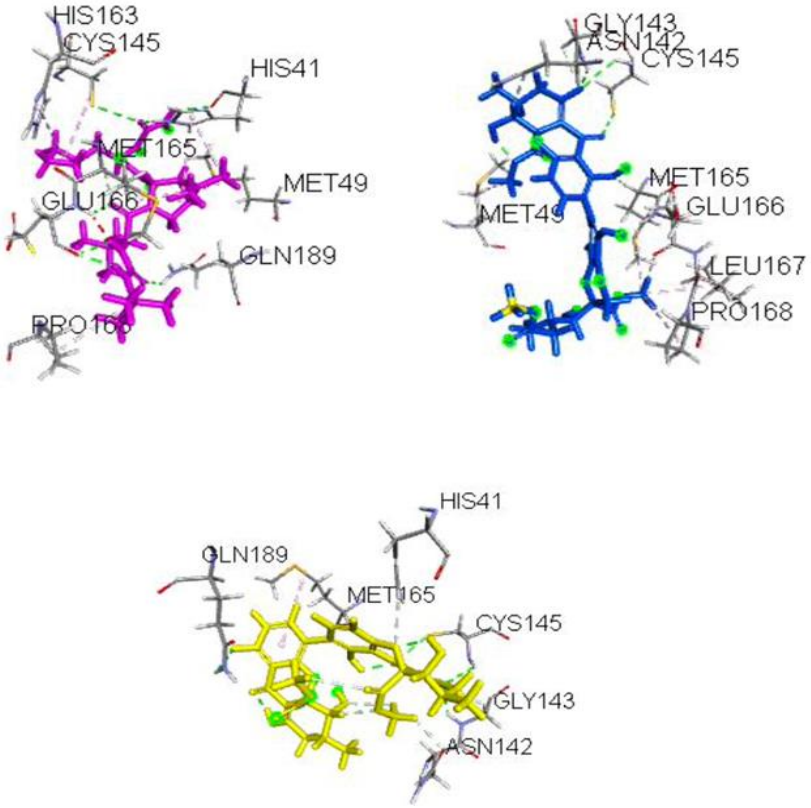


**Figure 3.** Docking poses of Boceprevir (violet, upper left), CMNPD26286 (blue, upper right), and CMNPD26369 (yellow, bottom) with SARS-CoV-2 main protease, highlighting key interacting residues.

In the ligand-based approach, ninety-eight CMNPD compounds surpassed the reference ligand; the top ten are shown in **Table 2**. The lead hit, CMNPD26369 (penicillixanthone B), had a binding energy of –471.0 kcal/mol and interacted via hydrogen bonds with Gly143, Cys145, and Gln189, as well as π–π-π-alkyl interactions with Met165. The ligand-based approach also identified triphloroethohydroxycarmalol (CMNPD4737), penicillixanthone A (CMNPD26368), versixanthone I (CMNPD28909), and versixanthone D (CMNPD26284) as high-ranking candidates with favorable binding profiles. Both top hits (versixanthone F and penicillixanthone B) and boceprevir share a key hydrogen bond with Cys145, a catalytic residue whose covalent modification can inhibit protease activity (Mengist *et al*., 2021). However, of the two lead compounds, only CMNPD26369 emerged as a common top hit in both the structure- and ligand-based screenings. Consequently, only the 29 compounds identified by both approaches were advanced to ADMET filtering.

**Table 2.** Top 5 ligand-based hits with their structures, binding energies, and fit values.

| Index | Compound ID | Structure* | Binding Energy (kcal/mol) | Fit Value (Rigid) | Fit Value (Flexible) |
|---|---|---|---|---|---|
| **1** | CMNPD26369 | 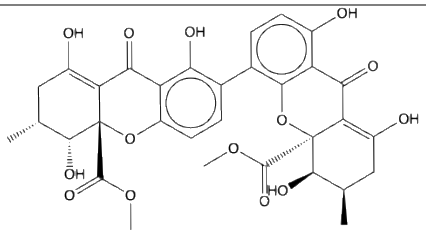 | –471.0 | 2.80 | 2.98 |

| | | | | | |
|---|---|---|---|---|---|
| **2** | CMNPD4737 | 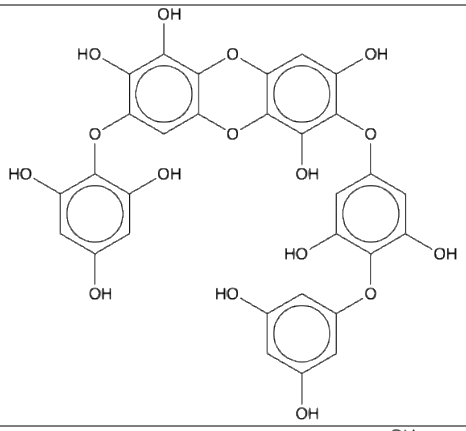 | –452.4 | 2.62 | 2.94 |
| **3** | CMNPD26368 | 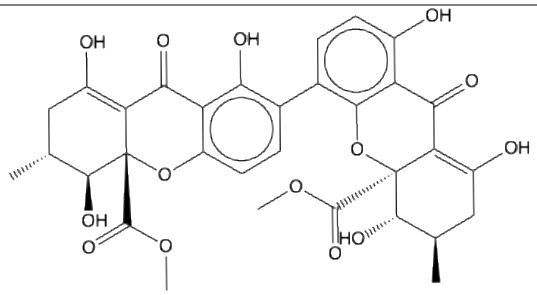 | –435.6 | 2.62 | 2.96 |
| **4** | CMNPD28909 | 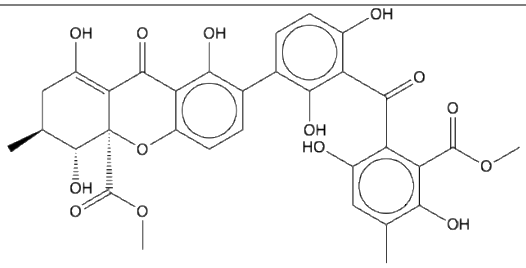 | –434.3 | 2.69 | 2.93 |
| **5** | CMNPD26284 | 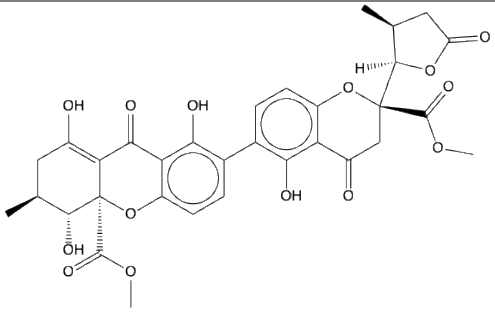 | –429.7 | 2.62 | 2.92 |

*ADME–Tox Evaluation*

ADMET properties were assessed early to identify potential pharmacokinetic or toxicity issues, as these account for ~50% of drug-development failures (Arodola & Soliman, 2017). SwissADME predicted physicochemical parameters, lipophilicity, water solubility, pharmacokinetics, and medicinal chemistry alerts (Daina *et al*., 2017). Lipinski's Rule of Five was not strictly applied, as marine natural products often violate these rules yet remain drug-like (Ganesan, 2008). Discovery Studio ADMET Descriptors predicted human intestinal absorption, aqueous solubility, CYP2D6 inhibition, hepatotoxicity, and plasma-protein binding. TOPKAT models estimated rodent carcinogenicity, Ames mutagenicity, developmental toxicity, and aerobic biodegradability. These combined evaluations guided the selection of promising candidates from the common top hits of both screening strategies.

The common top-hit compounds identified by both the structure-based and ligand-based screenings were first subjected to ADMET filtering using lipophilicity (logP 0–3), PAINS alert (0), and synthetic accessibility (≤6) as criteria. Lipophilicity within this range supports membrane permeability and drug potency, while allowing room for future synthetic modifications to improve absorption (Waring, 2010). The PAINS filter removes compounds prone to false positives in high-throughput screens (Baell & Holloway, 2010), and a synthetic accessibility score ≤6 ensures reasonable ease of production (Ertl & Schuffenhauer, 2009).

From 29 common compounds, only three—CMNPD22635 (Purealin D), CMNPD26181 (pseudogymnoascin B), and CMNPD26180 (pseudogymnoascin A)—passed these filters **(Figure 4)**. Although these marine natural products exhibited desirable lipophilicity, PAINS, and synthetic accessibility values, they showed several unfavorable ADME-Tox traits, including hepatotoxicity, very low intestinal absorption, high plasma-protein binding (>95% for CMNPD26181 and CMNPD26180), and developmental toxicity potential. These limitations suggest that further optimization, such as structural modification or dosage adjustment, would be needed to advance these compounds as leads.

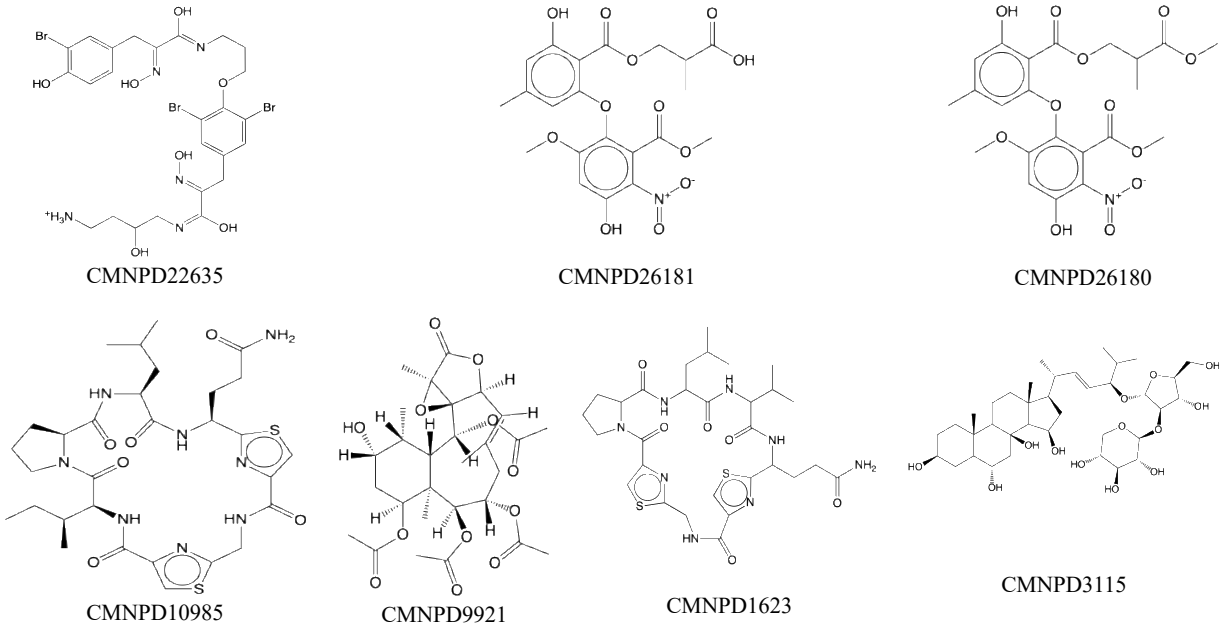


**Figure 4.** Structures of top candidates after ADMET screening.

To identify additional promising candidates, the full sets of structure-based (88) and ligand-based (98) hits were separately screened for non-hepatotoxicity, non-CYP2D6 inhibition, plasma-protein binding <90%, and negative TOPKAT toxicity predictions. This yielded four more favorable compounds: CMNPD10985 (homodolastatin 3) and CMNPD9921 (excavatolide C) from the ligand-based set, and CMNPD1623 (dolastatin 3) and CMNPD3115 (22,23-didehydrohalityloside E) from the structure-based set. All of these compounds showed low intestinal absorption and high synthetic accessibility scores, suggesting that chemical production would be difficult, despite their acceptable lipophilicity, PAINS scores, and overall toxicity profiles. Nevertheless, as natural products, they could still be obtained through targeted extraction if suitable protocols are developed.

## Conclusion

This study successfully applied an integrated CADD workflow—combining structure-based and ligand-based pharmacophore modelling, virtual screening, molecular docking, and ADME–Tox assessment—to identify promising SARS-CoV-2 $M^{pro}$ inhibitors from marine natural products. Several compounds, notably versixanthone F and penicillixanthone B, demonstrated strong predicted binding affinities and key interactions with catalytic residue Cys145. Although only three common hits passed initial drug-likeness filters, their unfavorable ADME–Tox profiles highlight the need for structural optimization. Additional unique hits from each screening approach, including homodolastatin 3, excavatolide C, dolastatin 3, and 22,23-didehydrohalityloside E, exhibited more favorable toxicity predictions and represent viable leads. Overall, the results underscore marine natural products as a rich source of potential antiviral scaffolds and provide a set of prioritized compounds for future chemical modification, *in vitro* validation, and preclinical development toward novel COVID-19 therapeutics.

**Acknowledgments:** The authors used ChatGPT (OpenAI, San Francisco, CA, USA) to help improve sentence clarity.

**Conflict of interest:** None

**Financial support:** The authors gratefully acknowledge the financial support of the University of the Philippines Manila through its Research Dissemination Grant (SDG).

**Ethics statement:** This study involved only computational analyses of publicly available and computer-generated data and did not include any experiments on humans or animals. Therefore, ethics approval and informed consent were not required.

## References

Arodola, O. A., & Soliman, M. (2017). Quantum mechanics

implementation in drug-design workflows: does it really help? *Drug Design, Development and Therapy, 11*, 2551–2564. doi:10.2147/DDDT.S155133

Baell, J. B., & Holloway, G. A. (2010). New substructure filters for removal of pan assay interference compounds (pains) from screening libraries and for their exclusion in bioassays. *Journal of Medicinal Chemistry, 53*(7), 2719–2740. doi:10.1021/jm901137j

Billones, J. B., Carrillo, M. C. O., Organo, V. G., Macalino, S. J. Y., Emnacen, I. A., & Sy, J. B. A. (2013). Virtual screening against *Mycobacterium tuberculosis* lipoate protein ligase B (MtbLipB) and in silico ADMET evaluation of top hits. *Oriental Journal of Chemistry, 29*(4), 1457–1468. doi:10.13005/ojc/290423

Billones, J. B., Carrillo, M. C. O., Organo, V. G., Macalino, S. J. Y., Sy, J. B. A., Emnacen, I. A., Clavio, N. A. B., & Concepcion, G. P. (2016). Toward antituberculosis drugs: in silico screening of synthetic compounds against *Mycobacterium tuberculosis* L, D-transpeptidase 2. *Drug Design, Development and Therapy, 10*, 1147–1157. doi:10.2147/DDDT.S97043

Caly, L., Druce, J. D., Catton, M. G., Jans, D. A., & Wagstaff, K. M. (2020). The FDA-approved drug ivermectin inhibits the replication of SARS-CoV-2 in vitro. *Antiviral Research, 178*, 104787. doi:10.1016/j.antiviral.2020.104787

Cascella, M., Rajnik, M., Aleem, A., Dulebohn, S. C., & Di Napoli, R. (2023). Features, evaluation, and treatment of coronavirus (COVID-19). *StatPearls [Internet]*. https://www.ncbi.nlm.nih.gov/books/NBK554776/

Çorbacıoğlu, Ş. K., & Aksel, G. (2023). Receiver operating characteristic curve analysis in diagnostic accuracy studies: a guide to interpreting the area under the curve value. *Turkish Journal of Emergency Medicine, 23*(4), 195–198. doi:10.4103/tjem.tjem_182_23

Cosconati, S., Forli, S., Perryman, A. L., Harris, R., Goodsell, D. S., & Olson, A. J. (2010). Virtual screening with AutoDock: theory and practice. *Expert Opinion on Drug Discovery, 5*(6), 597–607. doi:10.1517/17460441.2010.484460

Costa, L. A., Eiro, N., Vaca, A., & Vizoso, F. J. (2022). Advanced microscopy and cell culture techniques in regenerative endodontics. *Asian Journal of Periodontics and Orthodontics, 2*, 42–46. doi:10.51847/ExCWvexPbC

Daina, A., Michielin, O., & Zoete, V. (2017). SwissADME: a free web tool to evaluate pharmacokinetics, drug-likeness, and medicinal chemistry friendliness of small molecules. *Scientific Reports, 7*, 42717. doi:10.1038/srep42717

Dipalma, G., Inchingolo, A. D., Fiore, A., Balestriere, L., Nardelli, P., Casamassima, L., Venere, D. D., Palermo, A., Inchingolo, F., & Inchingolo, A. M. (2022). Comparative effects of fixed and clear aligner therapy on oral microbiome dynamics. *Asian Journal of Periodontics and Orthodontics, 2*, 33–41. doi:10.51847/mK28wdKCIX

Ertl, P., & Schuffenhauer, A. (2009). Estimation of the synthetic accessibility score of drug-like molecules based on molecular complexity and fragment contributions. *Journal of Cheminformatics, 1*, 8. doi:10.1186/1758-2946-1-8

Fletcher, R., & Reeves, C. M. (1964). Function minimization by conjugate gradients. *The Computer Journal, 7*(2), 149–154. doi:10.1093/comjnl/7.2.149

Fu, L., Ye, F., Feng, Y., Yu, F., Wang, Q., Wu, Y., Zhao, Z., Sun, H., Huang, B., Niu, P., et al. (2020). Both Boceprevir and GC376 efficaciously inhibit SARS-CoV-2 by targeting its main protease. *Nature Communications, 11*, 4417. doi:10.1038/s41467-020-18233-x

Ganesan, A. (2008). The impact of natural products upon modern drug discovery. *Current Opinion in Chemical Biology, 12*(3), 306–317. doi:10.1016/j.cbpa.2008.03.016

García, E., & Jaramillo, S. (2023). Telescopic retention in prosthodontics: a digital approach for enhanced patient outcomes. *Asian Journal of Periodontics and Orthodontics, 3*, 25–29. doi:10.51847/zpD7lrfE1t

Gaudêncio, S. P., & Pereira, F. (2020). A computer-aided drug design approach to predict marine drug-like leads for SARS-CoV-2 main protease inhibition. *Marine Drugs, 18*(12). doi:10.3390/md18120633

Gurung, A. B., Ali, M. A., Lee, J., Farah, M. A., & Al-Anazi, K. M. (2021). An updated review of computer-aided drug design and its application to COVID-19. *BioMed Research International, 853056*, 1–18. doi:10.1155/2021/8853056

Iheagwam, F. N., & Rotimi, S. O. (2020). Computer-aided analysis of multiple SARS-CoV-2 therapeutic targets: identification of potent molecules from African medicinal plants. *Scientifica, 878410*, 1–25. doi:10.1155/2020/1878410

Jackson, C. B., Farzan, M., Chen, B., & Choe, H. (2022). Mechanisms of SARS-CoV-2 entry into cells. *Nature Reviews Molecular Cell Biology, 23*, 3–20. doi:10.1038/s41580-021-00418-x

Lyu, C., Chen, T., Qiang, B., Liu, N., Wang, H., Zhang, L., & Liu, Z. (2021). CMNPD: a comprehensive marine natural products database towards facilitating drug discovery from the ocean. *Nucleic Acids Research, 49*(D1), D509–D515. doi:10.1093/nar/gkaa763

Macip, G., Garcia-Segura, P., Mestres-Truyol, J., Saldivar-Espinoza, B., Pujadas, G., & Garcia-Vallvé, S. (2022). A review of the current landscape of SARS-CoV-2 main protease inhibitors: Have we hit the bullseye yet? *International Journal of Molecular Sciences, 23*(1), 259. doi:10.3390/ijms23010259

Maia, E. H. B., Assis, L. C., de Oliveira, T. A., da Silva, A. M., & Taranto, A. G. (2020). Structure-based virtual screening: from classical to artificial intelligence. *Frontiers in Chemistry, 8*. doi:10.3389/fchem.2020.00343

Meng, X. Y., Zhang, H. X., Mezei, M., & Cui, M. (2011). Molecular docking: a powerful approach for structure-based drug discovery. *Current Computer Aided Drug Design, 7*(2), 146–157. doi:10.2174/157340911795677602

Mengist, H. M., Dilnessa, T., & Jin, T. (2021). Structural basis of potential inhibitors targeting SARS-CoV-2 main protease. *Frontiers in Chemistry, 9*, 622898. doi:10.3389/fchem.2021.622898

Ramos-Guzmán, C. A., Ruiz-Pernía, J. J., & Tuñón, I. (2020). Unraveling the SARS-CoV-2 main protease mechanism using multiscale methods. *ACS Catalysis, 10*(21), 12544–12554. doi:10.1021/acscatal.0c03420

Reina, J., & Iglesias, C. (2022). Nirmatrelvir plus ritonavir (Paxlovid) is a potent SARS-CoV-2 3CLpro protease

inhibitor combination. *Revista Española de Quimioterapia, 35*(3), 236–240. https://pubmed.ncbi.nlm.nih.gov/35183067/

Sharma, V., Wakode, S., & Kumar, H. (2021). Chapter 2 - Structure- and ligand-based drug design. *Chemoinformatics and Bioinformatics in the Pharmaceutical Sciences*, 27–53. doi:10.1016/b978-0-12-821748-1.00004-x

Shehroz, M., Zaheer, T., & Hussain, T. (2020). Computer-aided drug design against spike glycoprotein of SARS-CoV-2 to aid COVID-19 treatment. *Heliyon, 6*(10), e05278. doi:10.1016/j.heliyon.2020.e05278

Stoev, A. N., Pavlova, Z., & Vasileva, I. M. (2023). Innovative use of 3D-printed metal appliances for orthodontic treatment of palatally impacted maxillary canines. *Asian Journal of Periodontics and Orthodontics, 3*, 44–52. doi:10.51847/T0fTuJw29g

Sugimori, T., Yamaguchi, M., Kikuta, J., Shimizu, M., & Negishi, S. (2022). The biomechanical and cellular response to micro-perforations in orthodontic therapy. *Asian Journal of Periodontics and Orthodontics, 2*, 1–15. doi:10.51847/Z9adSJ59rj

Tomar, V., Mazumder, M., Chandra, R., Yang, J., & Sakharkar, M. K. (2019). Small molecule drug design. In *Encyclopedia of Bioinformatics and Computational Biology, 3*, 741–760. doi:10.1016/b978-0-12-809633-8.20157-x

Waring, M. J. (2010). Lipophilicity in drug discovery. *Expert Opinion on Drug Discovery, 5*(3), 235–248. doi:10.1517/17460441003605098

Wu, G., Robertson, D. H., Brooks, C. L., 3rd, & Vieth, M. (2003). Detailed analysis of grid-based molecular docking: a case study of CDOCKER—A CHARMm-based MD docking algorithm. *Journal of Computational Chemistry, 24*(13), 1549–1562. doi:10.1002/jcc.10306

Yang, S. Y. (2010). Pharmacophore modeling and applications in drug discovery: Challenges and recent advances. *Drug Discovery Today, 15*(11–12), 444–450. doi:10.1016/j.drudis.2010.03.013

Yurievna, L. E., Mikhailovich, P. V., Tokhiriyon, B., Nikolaevna, D. N., Anatolyevna, P. G., & Yurievich, L. N. (2023). A comparative evaluation of "Cerafill" and "iRoot" bioceramic sealers: Mechanical and chemical insights. *Asian Journal of Periodontics and Orthodontics, 3*, 12–17. doi:10.51847/xwOhbZsqp0

Zhang, L., Lin, D., Sun, X., Curth, U., Drosten, C., Sauerhering, L., Becker, S., Rox, K., & Hilgenfeld, R. (2020). Crystal structure of SARS-CoV-2 main protease provides a basis for design of improved α-ketoamide inhibitors. *Science, 368*(6489), 409–412. doi:10.1126/science.abb3405

Zhao, D., Xue, K., Meng, J., Hu, M., & Tan, X. (2022). Root canal treatment in posterior teeth: implications for orthodontic mechanics and stability. *Asian Journal of Periodontics and Orthodontics, 2*, 27–32. doi:10.51847/cTjogcutDJ